on the subject. However, some unexplained issues remain which were impossible to define experimentally, the major being the inability to perform a detailed examination of the action of integrity reinforcement rods in the connection. In this case it was concluded that the deformation and load-bearing capacity they can provide would be revealed by means of a numerical simulation.

3 The numerical model

The computer simulation of the action of integrity reinforcement bars in experimental models was conducted using *ANSYS*. The numerical model was developed with reference to the experience of the authors of papers [6, 7, 8, 9,10] in the fields of: utilization of linear and non-linear material models, assuming the different-shaped type of finite elements, selection of their size for meshing, use of iterative calculation methods. The author's own analyses were included in publications [11, 12, 13]. They referred to the simulation of the behavior of integrity reinforcement bars in a state of significant deformation, pointing at numerous relevant factors which should be taken into account when mapping real phenomena. The analyses pertained both to technical aspects of modelling the structure of individual elements of the building and physical aspects that stem from modelling of steel and concrete properties.

a)

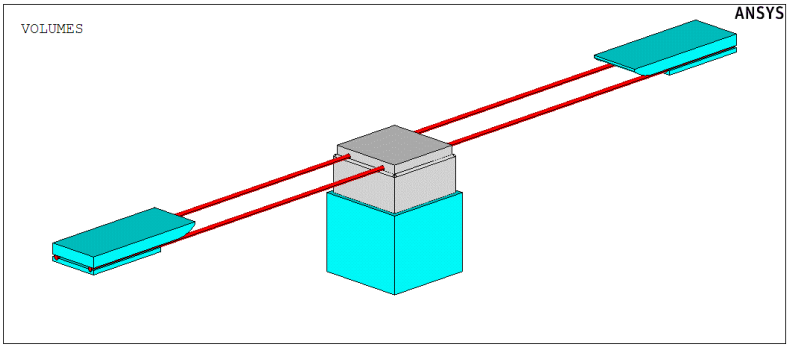

b)

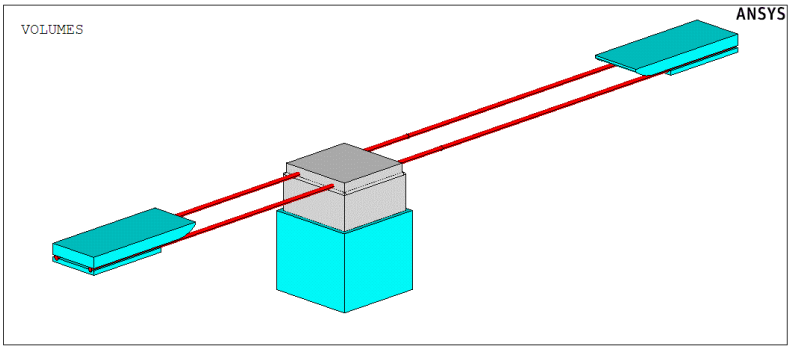

Fig. 1. Types of analyzed numerical models with regard to the column positioned: a) axially, b) eccentrically.

The numerical model consisted of a column element (Fig. 1) with two integrity reinforcement bars passing through. The ends of those rods were immobilized in supports. The load was applied at the base of the column, taking into account its location: axial and eccentric. View of the simplified model with the description of elements and materials applied can be found in Fig. 2. The detailed description of the numerical model and its verification based on experimental research is included in papers [11, 12, 13].

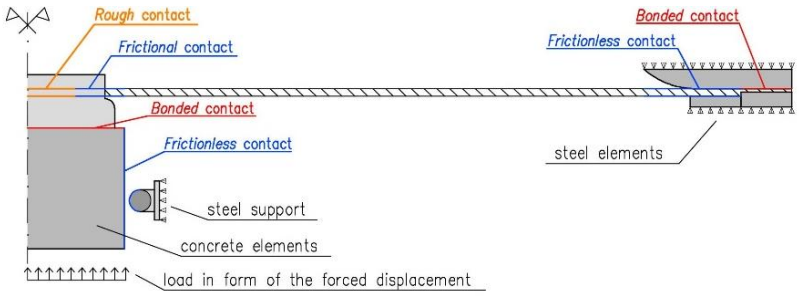

Fig. 2. Scheme of the numerical model – division into elements, contact between elements.

The developed numerical model made it possible to carry out a detailed analysis of the distribution of stresses in individual parts of the integrity reinforcement bar. Moreover, the load-displacement-force dependence was specified. It served as the basis for determining the maximum value of the loading force accompanying the rupture of integrity reinforcement bars. The calculation results were presented and discussed in papers [11, 12, 13], along with the reference to guidelines included in standards.

To be able to generalize the analysis conclusions, considerations were necessary for connections with different types of reinforcing steel and diameters of integrity reinforcement bars.

4 The scope of numerical analysis

The analysis included the change of values defining the most important parameters of reinforcing steel properties (Fig. 3). Also, parameters directly related to the geometry of the slab-column connection itself were considered (Fig. 4).

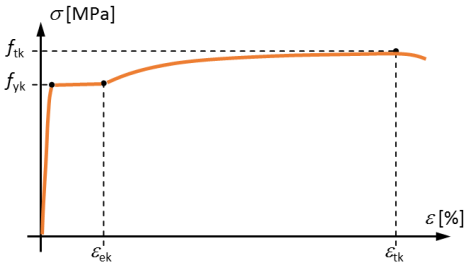

Fig. 3. Designation of parameters defining the σ–ε relation with strengthening.

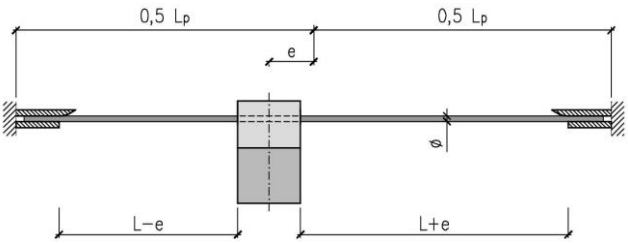

Fig. 4. Designation of parameters describing the bars of integrity reinforcement.

In numerical simulations, the following parameters defining the σ-ε dependence curve of reinforcement steel were assumed for analysis: value of strain at the end of the yield plateau ε_{ek} and value of strain at the time of rupture ε_{tk}, at a fixed yield strength of steel f_{yk} and ratio of strength against rupture f_{yt} and yield strength f_{yk}. In addition, the parameters

defining integrity reinforcement bars were considered: location of load action on bars, length of reinforcing bars between attachment points and diameter of the bars.

Parameters describing the σ–ε curve (Fig. 3) were determined according to the following assumptions. Three values of strain at rupture ε_{tk} were defined: 7.5%, 15% and 20% (marked with A, B and C respectively) and three values of strain at strengthening ε_{ek}, of 1%, 3% and 5% (marked with 1, 2 and 3 respectively). In total, 9 curves were obtained. Each of them was considered with the yield strength f_{yk} of 500 MPa and steel strength against rupture f_{tk} determined on the basis of strengthening factor Δ of 1.15. The graphs σ–ε included in calculations are presented in Fig. 5. The diversification of individual parameters assumed in the analysis corresponded to the requirements which have to be fulfilled by reinforcing steel – class C according to EC2 [2].

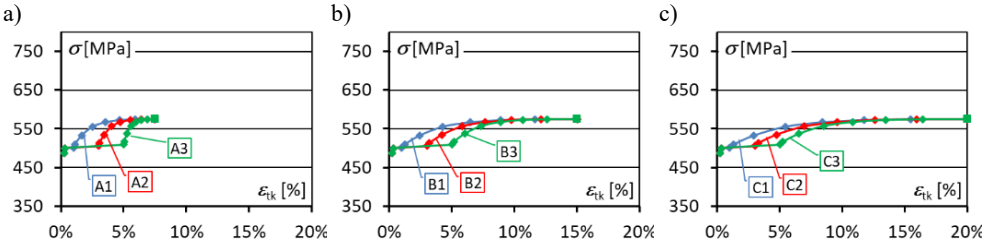

Fig. 5. Summary of curves defining the σ–ε relation according to various f_{yk} = 500 MPa and f_{tk} = 1.15 f_{yk}: a) ε_{tk} =7.5%, b) ε_{tk} =15%, c) ε_{tk} =20%.

Among the parameters describing integrity reinforcement bars, the length of bars and location of load action on them were considered primarily. The numerical calculations were carried out for 1170 mm long bars ø16 mm, between their attachment points in supports. Two different positions of the column were taken into account: halfway through the span of the bars and at the offset corresponding to 285 mm. This allowed to maintain proportions between the eccentric position of the column and the bar length, which has been taken into account in the analysis.

Numerical simulations were carried out using two types of models: UU-I and UU-II (Fig. 1), with the consideration of the above-mentioned parameters. Because of a considerable number of results and analogical conclusions derived, the results presented below are limited to introducing the most important parameters only. The scope of the analysis focused mainly on comparing the load-bearing capacity of the integrity reinforcement bars, based on the maximum value of force F_{max} acting on the connection directly before the rupture of the first bar, and the vertical displacement of column a_{max} corresponding to force F_{max}.

5 Results of numerical calculations

Based on the simulations carried out, information was obtained about the change in the force value affecting the connection, depending on the forced vertical displacement of the column. Graphs showing the force-displacement relationship are given in Fig. 6. Summary of forces F_{max} directly preceding the rupture of the bar, along with the corresponding displacement of column a_{max}, is presented in Table 1.

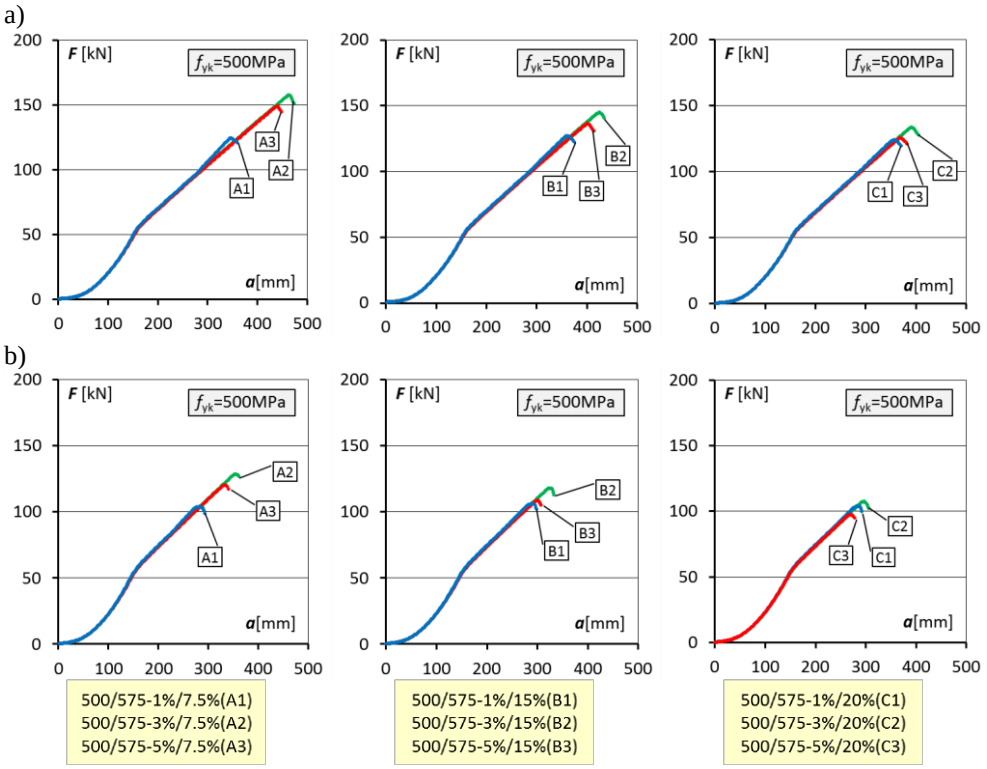

Fig. 6. Diagrams of the force-displacement relation for f_{tk}=1.15 f_{yk} and f_{yk}=500 MPa, taking into account the following eccentric position of the column: a) 0 mm, b) 285 mm.

Table 1. Summary of values F_{max} and a_{max} , taking into account bars of f_{tk}/f_{yk}=1.15 and f_{yk}=500 MPa, with the following eccentric position of the column: 0 mm and 285 mm.

Parameters		**σ–ε dependence curve**								
		A1	**A2**	**A3**	**B1**	**B2**	**B3**	**C1**	**C2**	**C3**
e	**ε_{ek} [%]**	1%	3%	5%	1%	3%	5%	1%	3%	5%
[mm]	**ε_{tk} [%]**	7.5%	7.5%	7.5%	15%	15%	15%	20%	20%	20%
0	F_{max} [kN]	124.1	157.5	148.9	126.4	144.5	135.9	123.6	133.2	125.0
	a_{max} [mm]	347	465	440	362	425	401	357	392	369
285	F_{max} [kN]	103.4	128.3	120.0	105.8	117.7	108.1	103.7	107.2	97.2
	a_{max} [mm]	280	354	333	291	327	303	287	299	273

The greatest load-bearing capacity of the connection was obtained in the model in which the relationship σ–ε according to the A2 curve was assumed, where the length of the plastic shelf corresponded to the strain at strengthening ε_{ek}=3%, and the maximum steel strain at rupture was ε_{tk}=7.5% (Fig. 7). Also, in this case the highest value of column displacement, occurring at the at rupture of bar was obtained (Fig. 8). Values of F_{max} forces between individual models differed to 21.5% at the axial location of the column. However, in models

with a column shifted on the eccentric they amounted to 24.2% and 25.8% respectively. Differences in the value of displacement of the column amax obtained for individual models did not exceed 26%. Thus, the values of the strain ε_{ek} and ε_{ek} characterizing the reinforcing steel had a significant impact on the results obtained.

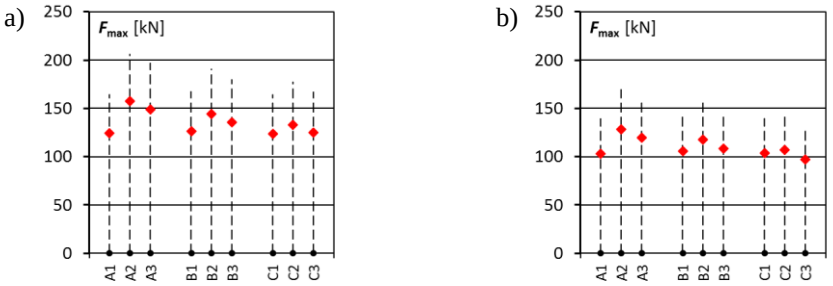

Fig. 7. Summary of values of F_{max} forces for f_{tk}=1.15 f_{yk} and f_{yk}=500 MPa, taking into account the following eccentric position of the column: a) 0 mm, b) 285 mm.

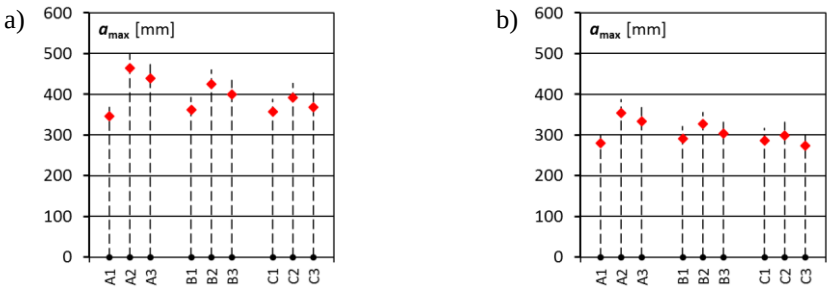

Fig. 8. Summary of values of a_{max} column displacements for f_{tk}=1.15 f_{yk} and f_{yk}=500 MPa, taking into account the following eccentric position of the column: a) 0 mm, b) 285 mm.

Based on the value of column displacements a_{max}, the values of bar inclination angles α_{max} were determined, relative to their original horizontal position (Table 2). The values of the bar inclination angle α_{max} ranged from 16° to 21° in models with an axially located column, while from 17° to 22° with its displacement on the eccentric (Fig. 9). The relative deformation of the bars ε_{max} at the length between the cross-sections in which they were bent was also determined (Table 2). In the ruptured bar, its value ranged from 4.5% to 7.4%. Slightly higher values of strain ε_{max} occurred in the case of models in which ε_{tk}=7.5% (models according to curves A1, A2 and A3) than in the others (Fig. 10). At the eccentric position of the column, the deformation of the longer bar reached a maximum value of 2.5%, with an eccentric equal to 285 mm.

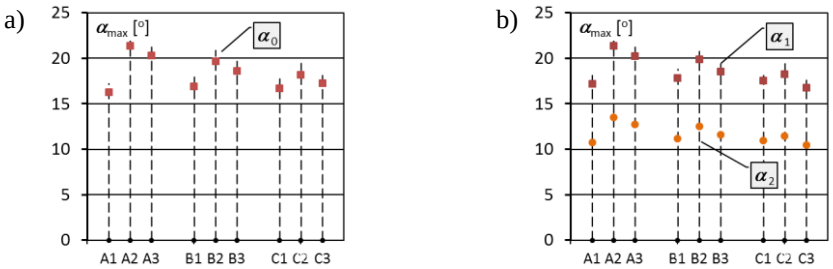

Fig. 9. Summary of values of α_{max} bar inclination angles for f_{tk}=1.15 f_{yk} and f_{yk}=500 MPa, taking into account the following eccentric position of the column: a) 0 mm, b) 285 mm.

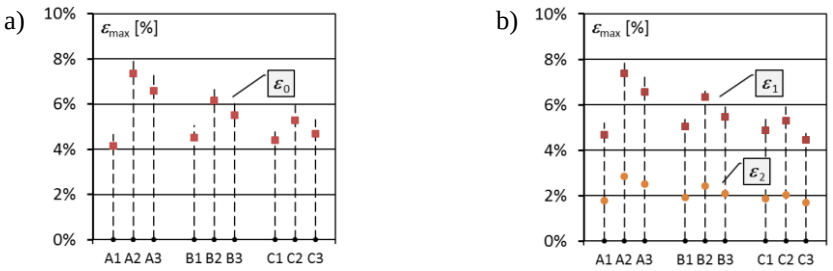

Fig. 10. Summary of values of ε_{max} bar strains for f_{tk}=1.15 f_{yk} and f_{yk}=500 MPa, taking into account the following eccentric position of the column: a) 0 mm, b) 285 mm.

Table 2. Summary of values α_{max} and ε_{max}, at f_{tk}=1.15 f_{yk} and f_{yk}=500 MPa - models with eccentric position of the column equal 0 mm and 285 mm.

Parameters		**σ–ε dependence curve**								
		A1	**A2**	**A3**	**B1**	**B2**	**B3**	**C1**	**C2**	**C3**
e	**ε_{ek} [%]**	1%	3%	5%	1%	3%	5%	1%	3%	5%
[mm]	**ε_{tk} [%]**	7.5%	7.5%	7.5%	15%	15%	15%	20%	20%	20%
0	$\alpha_{1,max}$ [°]	16.2	21.3	20.3	16.9	19.6	18.6	16.7	18.2	17.2
	$\varepsilon_{1,max}$ [%]	4.15	7.36	6.60	4.51	6.17	5.51	4.40	5.27	4.70
285	$\alpha_{1,max}$ [°]	17.2	21.4	20.2	17.8	19.9	18.5	17.6	18.3	16.8
	$\alpha_{2,max}$ [°]	10.8	13.5	12.7	11.2	12.5	11.6	11.0	11.4	10.5
	$\varepsilon_{1,max}$ [%]	4.68	7.38	6.55	5.04	6.33	5.46	4.89	5.30	4.45
	$\varepsilon_{2,max}$ [%]	1.79	2.84	2.52	1.93	2.43	2.09	1.87	2.03	1.70

5.1 Changes strain at strengthening

In the case of models in which the relationship σ–ε, was adopted, where the length of the plastic shelf was 1% (models according to the curve A1, B1 and C1), the load capacity of the connection was at the same level, regardless of the value of strain at rupture ε_{tk} (Fig. 11). The differences in the F_{max} force values ranged from 0.8% to 2.3%, regardless of the column position.

In the models in which ε_{ek}=3% (models according to curve A2, B2 and C2), the highest load-bearing capacity was obtained when the ε_{tk} value was assumed equal to 7.5% (model according to curve A2). At ε_{tk} of 15% (model according to the B2 curve), the load-bearing capacity of the connection was reduced by 8.7%÷10.6%, while at ε_{tk}=20% (model according to the C3 curve) it was lower by a further 7.4%÷10.1%.

Similar observations concerned the models in which ε_{ek}=5% (models according to curves A3, B3 and C3). Here, too, the largest load-bearing capacity of the connection was obtained at ε_{tk}=7.5% (model according to curve A3). The decrease of its value occurred by 9.6%÷13.3% and additionally by 7.9%÷10.4%, respectively, with ε_{tk} equal to 15% (model

according to curve B3) and 20% (model according to curve C3). In addition, the load-bearing carrying capacities of these connections were 3.4% to 4.6% lower compared to the corresponding models according to curves A2, B2 and C2. The above regularities occurred in both the axial and eccentric position of the column.

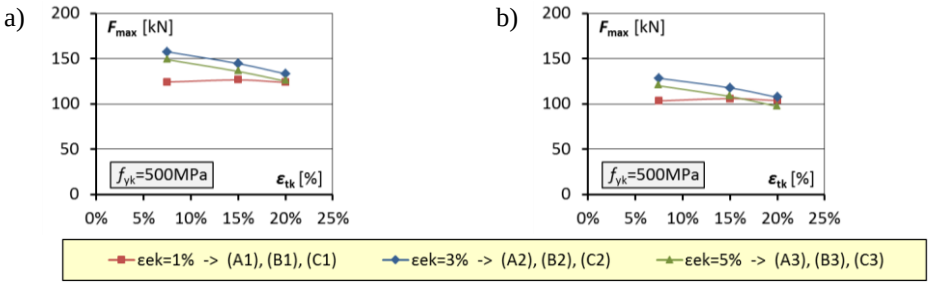

Fig. 11. Summary of values of F_{max} forces depending on the values of ε_{tk} strain for f_{tk}=1.15 f_{yk} and f_{yk} =500 MPa, taking into account the following eccentric position of the column: a) 0 mm, b) 285 mm.

Similar relationships were observed in the range of displacement of the column a_{max}, corresponding to the obtained values of forces F_{max} (Fig. 12).

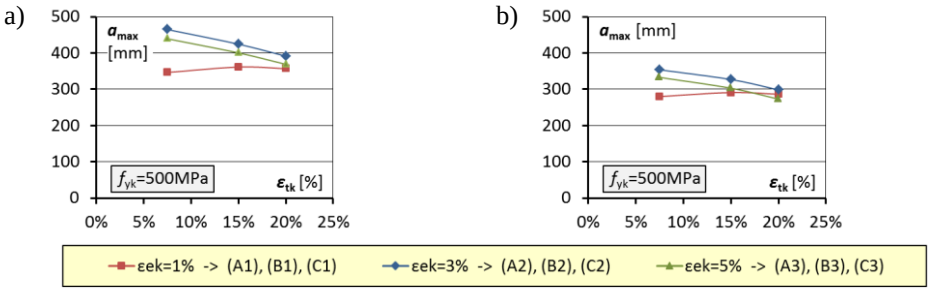

Fig. 12. Summary of values of a_{max} column displacements depending on the values of ε_{tk} strain for f_{tk}=1,15 f_{yk} and f_{yk}=500 MPa, taking into account the following eccentric position of the column: a) 0 mm, b) 285 mm.

5.2 Changes of maximum elongation at rupture

The highest load-bearing carrying of connection were obtained in models, in which in dependence σ–ε the strain at rupture ε_{tk} was assumed to be 7.5% (models according to curve A1, A2 and A3. Increasing its value caused a decrease of the load-bearing capacity of the connection (Fig. 13). In models in which the total elongation at rupture ε_{tk} was assumed to be 15% and 20%, the decrease of their load-bearing capacity was 9.1%÷10.6% and respectively 18.3%÷22.8% at ε_{ek}=3% (models according to B2 and B3 curve) and 9.6%÷13.3% and 19.1%÷25.6% respectively, with ε_{ek}=5% (models according to the C2 and C3 curves). However, at ε_{ek}=1% (models according to curve A1, B1 and C1), the load-bearing capacity of the connections remained at the same level, regardless of the total elongation ε_{tk}. The above regularities occurred regardless of the location of the column.

In the case of displacement of the column a_{max}, corresponding to the obtained values of forces F_{max}, analogous relationships occurred (Fig. 14).

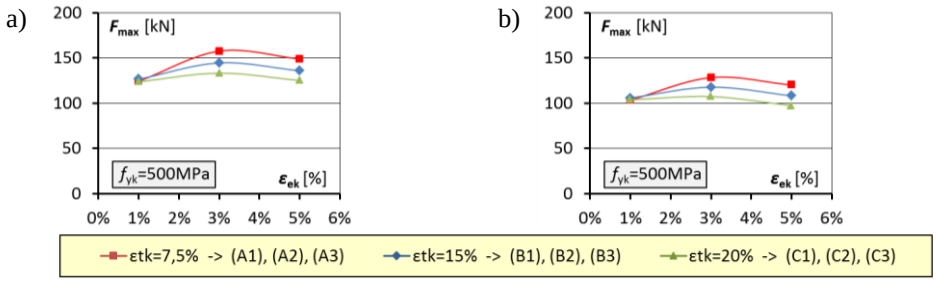

Fig. 13. Summary of values of F_{max} forces depending on the values of ε_{ek} strain for f_{tk}=1,15 f_{yk} and f_{yk}=500 MPa, taking into account the following eccentric position of the column: a) 0 mm, b) 285 mm.

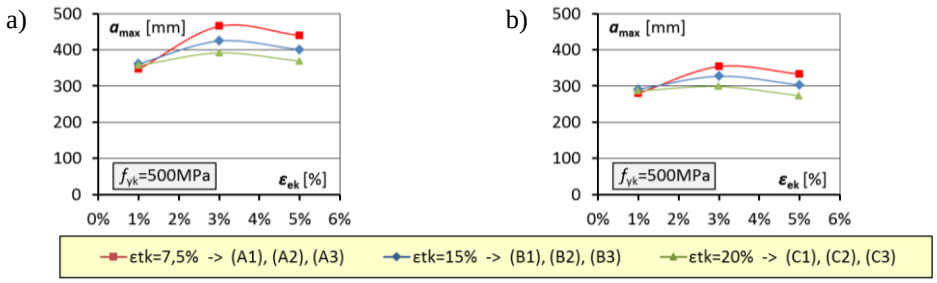

Fig. 14. Summary of values of a_{max} column displacements depending on the value of ε_{ek} strain for f_{tk}=1.15 f_{yk} and f_{yk}=500 MPa, taking into account the following eccentric position of the column: a) 0 mm, b) 285 mm.

5.3 Conclusions

At a strain ε_{ek} of 1%, the increase in strain value at break ε_{tk} from 7.5% to 20% did not change the load-bearing capacity of the connection, which remained at the same level. Increasing the value of strain ε_{ek} to 3% caused an increase in the load-bearing capacity of the connection, which was particularly visible at ε_{tk}=7.5%, and slightly smaller at ε_{tk}=15%. Further elongation of the plastic shelf no longer resulted in an increase in the value of F_{max}. On the contrary it was smaller than at ε_{ek}=3%. In addition, at ε_{tk}=20%, adopting different values of strain ε_{ek} did not practically affect the load-bearing capacity of the connection. At the same time, it was noticed that the differences in the maximum values of forces F_{max} obtained for individual models, with the eccentric position of the column, were smaller than with its axial position.

Increasing the strain at rupture ε_{tk} from 7.5% to 20% resulted in a reduction of the connection load-bearing capacity to 18.3%÷20.6%, wherein its size depending on the strain ε_{ek}. With a strain ε_{ek} equal to 1%, the change in the load-bearing capacity of the connection was practically zero, and with its increase to 3% and 5%, it was decreased.

6 Summary

The numerical analysis made it possible to determine the impact of the individual mechanical and geometric parameters of the reinforcing steel on the load bearing capacity of the integrity reinforcement, and thus on the post-punching load-bearing capacity of the slab-column connection. The analysis was carried out using the numerical model that had been verified with experimental research [11, 12, 13]. Among the parameters analyzed (yield strength

of reinforcing steel, ratio of strength against rupture f_{yt} and yield strength f_{yk}, value of strain at the end of the yield plateau, value of strain at the time of rupture, location of load action on bars, length of reinforcing bars between attachment points), the change of the diameter of the integrity reinforcement bars turned out to be the most important one. One of the main conclusions drawn from analysis was the observation that assuming the greater diameters of the integrity bars, and thus increasing the cross-section area of the reinforcement, did not have proportional impact on the increment of the load-bearing capacity of integrity reinforcement bars in a slab-column connection. The bigger the increase of the cross-section of bars A_{sb} became, the smaller the increase of maximum force value F_{max} was. This pointed at the reduction in the load-bearing capacity with regard to the diameter of the bars applied. The detailed analysis of stresses proved that the increase in the diameter of the bars was accompanied by the increased contribution of normal stresses resulting from the bending of the bar compared to normal stresses resulting from the axial tensioning of the bar.

References

1. EN 1991-1-7:2008 – Eurocode 1 - Actions on structures - Part 1-7: General actions - Accidental actions (2008)
2. PN-EN 1992-1-1:2008 – Eurocode 2: Design of concrete structures - Part 1-1: General rules and rules for buildings (2008)
3. W. Starosolski, B. Wieczorek, M. Wieczorek: *Technical Bulletin*, 6, Steel Quality Promotion Center, Warsaw (2015)
4. B. Wieczorek: *Procedia Engineering*, **57** (2013)
5. B. Wieczorek: *Applied Mechanics and Materials*, **837** (2016)
6. J. Cervenka, V.K. Papanikolaou: *International Journal of Plasticity*, **24**, 12 (2008)
7. O. Sucharda, J. Brozovsky, D. Mikolasek: *Key Engineering Materials*, **577-578** (2014)
8. K.J. Willam, T. Tanabe: Finite element analysis of reinforced concrete structures, ACI International, Special Publication SP-205 (2001)
9. K.J. Willam, E.P. Warnke: Proceedings of the International Association for Bridge and Structural Engineering, 19, ISMES, May 17-19, Bergamo, Italy (1975)
10. E.L. Wilson, R.L. Taylor, W.P. Doherty, J. Ghaboussi: Incompatible displacement models, Numerical and Computer Methods in Structural Mechanics, Academic Press Inc., New York & London (1973)
11. B. Wieczorek: Procedingds of 20th International Conference “Engineering Mechanics”, (2014)
12. B. Wieczorek: *Applied Mechanics and Materials*, **769** (2015)
13. B. Wieczorek: *Procedia Engineering*, **190** (2017)